We are IntechOpen, the world's leading publisher of Open Access books Built by scientists, for scientists

4,800
Open access books available

122,000
International authors and editors

135M
Downloads

Our authors are among the

154
Countries delivered to

TOP 1%
most cited scientists

12.2%
Contributors from top 500 universities

CLARIVATE ANALYTICS BOOK CITATION INDEX INDEXED

WEB OF SCIENCE™

Selection of our books indexed in the Book Citation Index in Web of Science™ Core Collection (BKCI)

Interested in publishing with us?
Contact book.department@intechopen.com

Numbers displayed above are based on latest data collected.
For more information visit www.intechopen.com

Chapter

On the Thermodynamic Consistency of a Two Micro-Structured Thixotropic Constitutive Model

Hilbeth P. Azikri de Deus and Mikhail Itskov

Abstract

The time-dependent rheological behavior of the thixotropic fluids is presented in various industrial fields (cosmetics, food, oil, etc.). Usually, a couple of equations define constitutive model for thixotropic substances: a constitutive equation based on linear viscoelastic models and a rate equation (an equation related to the micro-structural evolution of the substance). Many constitutive models do not take into account the micro-structural dependence of the shear modulus and viscosity in the dynamic principles from which are developed. The modified Jeffreys model (considering only one single micro-structure type) does not show this incoherence in its formulation. In this chapter, a constitutive model for thixotropic fluids, based on modified Jeffreys model, is presented with the addition of one more micro-structure type, besides of comments on some possible generalizations. The rheological coherence of this constitutive model and thermodynamic consistency are analyzed too. This model takes into account a simple isothermal laminar shear flows, and the micro-structures dynamics are relate to Brownian motion and de Gennes Reptation model via the Smoluchowski™s coagulation theory.

Keywords: thixotropic fluids, thermodynamic consistency, modified Jeffreys model

1. Introduction

The thixotropic substances are considered structured fluids and have a rheological behavior (time-dependent) guided by their structural nature [1–5]. In terms of models (constitutive systems), this behavior is represented by a couple of time-dependent equations. These equations connect the micro-structural characteristics to the rheological behavior. In many works, this system of equations is based on a qualitative way, without any formal justification on the physical principles. In this chapter, a different approach is presented based on some well-established physical principles (Smoluchowski's coagulation theory [6–10], Brownian motion [6–9] and de Gennes reptation model [8, 11, 12]).

The rheological properties evolution, in many thixotropy models [2, 5, 13–17], is presented, generically, in terms of a couple of equations, as follows:

$$\tau = \tau(\lambda, \dot{\gamma}), \text{ constitutive relationship based on linear viscoelastic models;} \quad (1)$$

$$\dot{\lambda} = \mathfrak{G}_{\dot{\gamma}}(\lambda, \dot{\gamma}), \text{ relation associated to the micro} - \text{structural evolution,} \quad (2)$$

where τ is the shear stress (from Cauchy stress measure), $\dot{\gamma}$ is the shear rate (infinitesimal strain measure), λ is the structural parameter (a positive scalar quantity associated to the structural level of substance) and $\mathfrak{G}_{\dot{\gamma}}$ is a functional form. In large number of works [5, 18–21], Eq. (1) is represented by a linear viscoelastic model/mechanism (Maxwell, Jeffreys, Kelvin-Voigt, etc.) or combinations of that (in parallel or in series). However, it exists a problem with these approaches, they do not consider, the time/micro-structural dependence of the shear modulus (G) and viscosity (η_μ and η_ν) in physical principles from which the constitutive equation system is obtained. Differently, the approach presented in [8] (the modified Jeffreys model) does not present this mistake, considering time/micro-structural evolution in the constitutive system development, and in this way, showing more coherence to represent thixotropic substances behavior.

Eqs. (1) and (2) connect micro-structural characteristic and viscoelasticity nature of the thixotropy. In the specialized literature, a considerable number of micro-structure types [22–29] can be found, although only one single micro-structure type is considered in the development of the modified Jeffreys model. In this way, it is natural to imagine that it can exist more than one micro-structure type in a same thixotropic substance. In this chapter, a new perspective in terms of constitutive approach for thixotropic substances, with apparent-yield-stress nature and based on the modified Jeffreys model [8], is presented in terms of two different types of micro-structure (i.e., two structural parameters), and some of their properties are investigated in a rheological and thermodynamic sense. In the presented approach, each micro-structure is associated to a specific mechanism considered in the model (Maxwell-like element in parallel with a pure viscous Newtonian-like element), that is, one micro-structure type is associated to the Maxwellian element and another one to the pure viscous element. In this way, it is important to stand out that each of them (mechanisms) can react, under the shear loads, in distinct (but integrated) forms one from the other.

Aiming to extend the modified Jeffreys model for two distinguished micro-structures, in the next sections, the constitutive model is formally presented in terms of equations, the analysis of its thermodynamics consistence is done, points related to the characterization of the transition region are discussed and some illustrative numerical simulations of rheological tests are presented as well.

2. Main ideas on two types of micro-structures approach

The approach proposed in this work is based on a Jeffreys model [8] for the thixotropic system representation. In this case, a sketch of the model (Maxwell element in parallel with viscous element) is presented in **Figure 1**.

It is important to point out the presence of two micro-structure types (λ_μ and λ_ν) that are intimately related to the behavior of the shear modulus $G = G(\lambda_\nu)$, and viscosity coefficients $\eta_\nu = \eta_\nu(\lambda_\nu)$ and $\eta_\mu = \eta_\mu(\lambda_\mu)$. In this way, under a certain shear load (τ), for the Maxwell element ($.\nu$), one has

$$\tau_\nu = \eta_\nu \dot{\gamma}_{\nu_v}; \quad (3)$$

$$\dot{\tau}_\nu = G\dot{\gamma}_{\nu_e} + \dot{G}\gamma_{\nu_e}, \quad (4)$$

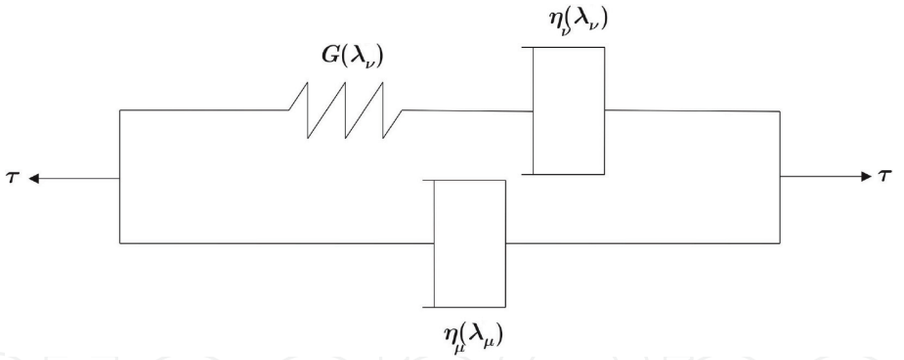

Figure 1.
Sketch of the two micro-structured thixotropic constitutive model.

where $\dot{\gamma}_{\nu_v}$ is the viscous strain rate and $\dot{\gamma}_{\nu_e}$ is the elastic strain rate, respectively, and the total strain rate for the Maxwell element is $\dot{\gamma}_\nu = \dot{\gamma}_{\nu_v} + \dot{\gamma}_{\nu_e}$. After some algebraic manipulation, it follows:

$$\dot{\gamma}_\nu = \frac{\tau_\nu}{\eta_\nu} + \frac{\dot{\tau}_\nu - \dot{G}\gamma_{\nu_e}}{G};$$

$$\therefore \eta_\nu \dot{\gamma}_\nu = \frac{\eta_\nu}{G}\dot{\tau}_\nu + \left(1 - \frac{\eta_\nu \dot{G}}{G^2}\right)\tau_\nu. \tag{5}$$

From the viscous element $(.\mu)$,

$$\dot{\gamma}_\mu = \frac{\tau_\mu}{\eta_\mu} \therefore \dot{\tau}_\mu = \dot{\eta}_\mu \dot{\gamma}_\mu + \eta_\mu \ddot{\gamma}_\mu, \tag{6}$$

and remembering that $\dot{\gamma} = \dot{\gamma}_\nu = \dot{\gamma}_\mu$ and $\tau = \tau_\nu + \tau_\mu \therefore \dot{\tau} = \dot{\tau}_\nu + \dot{\tau}_\mu$, one has

$$\dot{\tau} = G\dot{\gamma} - \frac{G}{\eta_\nu}\left(1 - \frac{\eta_\nu \dot{G}}{G^2}\right)\tau_\nu + \dot{\eta}_\mu \dot{\gamma} + \eta_\mu \ddot{\gamma}; \tag{7}$$

$$\therefore \frac{\eta_\nu}{G}\dot{\tau} + \left(1 - \frac{\eta_\nu \dot{G}}{G^2}\right)\tau = \left[\eta_\nu + \left(1 - \frac{\eta_\nu \dot{G}}{G^2}\right)\eta_\mu + \frac{\eta_\nu \dot{\eta}_\mu}{G}\right]\dot{\gamma} + \frac{\eta_\nu \eta_\mu}{G}\ddot{\gamma}. \tag{8}$$

It is important to stand out that the time variation of the shear modulus and the viscosity coefficient are taken into account, which is in agreement with the expected physical behavior of thixotropic fluids [8, 30, 31].

It is important to keep in mind the fact that the parameters λ_μ $(0 \le \lambda_\mu \le 1)$ and λ_ν $(0 \le \lambda_\nu \le 1)$ are used to characterize the structural level of the substance. The structural parameter closer to 1 implies highly building-up state of micro-structure, and when it is closer to 0, the micro-structure is close to a fully broken-down state, in respective mechanism $(.\nu$ or $.\mu)$. In this sense, it is presented the two micro-structures version of constitutive model based on the work [8].

$$\frac{\eta_\nu}{G}\dot{\tau} + \left(1 - \frac{\eta_\nu \dot{G}}{G^2}\right)\tau = \left[\eta_\nu + \left(1 - \frac{\eta_\nu \dot{G}}{G^2}\right)\eta_\mu + \frac{\eta_\nu \dot{\eta}_\mu}{G}\right]\dot{\gamma} + \frac{\eta_\nu \eta_\mu}{G}\ddot{\gamma}; \tag{9}$$

$$\frac{d\lambda_\nu}{dt} = \frac{1}{t_\nu}\left(k_\nu(1 - \lambda_\nu)^{\beta_\nu}\right) - \frac{\left(K_\nu^* \lambda_\nu^6 \theta\ddot{\gamma} + \tau_\nu\right)\lambda_\nu \dot{\gamma}}{\varsigma_\nu}; \tag{10}$$

$$\frac{d\lambda_\mu}{dt} = \frac{1}{t_\mu}\left(k_\mu\left(1-\lambda_\mu\right)^{\beta_\mu}\right) - \frac{\left(K_\mu^*\lambda_\mu^6\theta\ddot{\gamma} + \tau_\mu\right)\lambda_\mu\dot{\gamma}}{\varsigma_\mu}; \tag{11}$$

$$G(\lambda_\nu) = G_o\lambda_\nu^{\aleph}\exp\left(m{\lambda_\nu}^{-1}\right); \tag{12}$$

$$\eta_\nu(\lambda_\nu) = \eta_o\{\exp\left[(\alpha_1+\alpha_2)\lambda_\nu\right] - \exp\left(\alpha_2\lambda_\nu\right)\}; \tag{13}$$

$$\eta_\mu\left(\lambda_\mu\right) = \eta_o\exp\left(\alpha_3\lambda_\mu\right). \tag{14}$$

In this case, there are the following positive parameters: $\aleph$, k_ν, k_μ, β_ν, β_μ, t_ν, t_μ, G_o, m, ς_ν, ς_μ, K_ν^*, K_μ^*, η_o, α_1, α_2 and α_3. Some physical details related to these parameters can be found in [8, 32].

3. On the thermodynamic consistence

In this section, the thermodynamic consistence of constitutive model is analyzed in terms of the entropy-producing processes [33] associated with the concept of natural configuration [8, 34–36]. The main objective is to verify the consistence of the constitutive equation to the Clausius-Duhem inequality.

Figure 2 presents a sketch of the configurations spaces used in this approach for the body $\mathcal{B}$, where $\hat{k}_o(\mathcal{B})$ is the reference configuration, $\hat{k}_t(\mathcal{B})$ is the current/actual configuration, and $\hat{k}_{n(t)}(\mathcal{B})$ is a family of natural configurations. In isothermal process, one is supposed that $\hat{k}_{n(t)}(\mathcal{B}) = \hat{k}_{n(t)}(\mathcal{B})\left(\lambda_\mu, \lambda_\nu\right)$, where λ_μ and λ_ν are functions of the flow history. In this sense, it is assumed that the family of natural configurations can be parametrized by the structural level of the substance $(\lambda_\mu, \lambda_\nu)$. In this way, it has $\underline{\underline{F}}_{\hat{k}_o}$ (gradient of the motion from reference configuration to current configuration), $\underline{\underline{F}}_{\hat{k}_{n(t)}}$ (gradient of the motion from natural configuration to current configuration) and $\underline{\underline{F}}_{\hat{k}_o\to\hat{k}_{n(t)}}$ (gradient of the motion from reference configuration to natural configuration). In this way, denoting for each ξ_i-th relaxation mechanism.

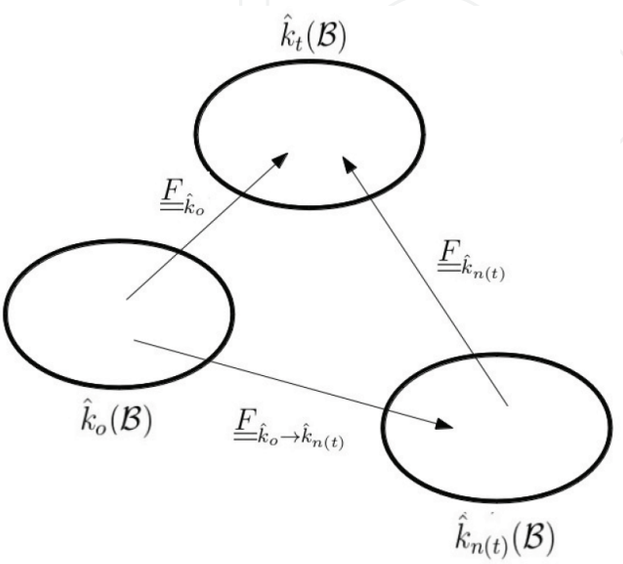

Figure 2.
Configuration spaces.

$$ {}^{\xi_i}\underline{\underline{B}}_{\hat{k}_{n(t)}} = {}^{\xi_i}\underline{\underline{F}}_{\hat{k}_{n(t)}} \, {}^{\xi_i}\underline{\underline{F}}^{T}_{\hat{k}_{n(t)}}; \tag{15} $$

$$ {}^{\xi_i}\underline{\underline{C}}_{\hat{k}_{n(t)}} = {}^{\xi_i}\underline{\underline{F}}^{T}_{\hat{k}_{n(t)}} \, {}^{\xi_i}\underline{\underline{F}}_{\hat{k}_{n(t)}}; \tag{16} $$

$$ {}^{\xi_i}\underline{\underline{L}}_{\hat{k}_{n(t)}} = {}^{\xi_i}\dot{\underline{\underline{F}}}_{\hat{k}_o \to \hat{k}_{n(t)}} \, {}^{\xi_i}\underline{\underline{F}}^{-1}_{\hat{k}_o \to \hat{k}_{n(t)}}; \tag{17} $$

$$ {}^{\xi_i}\underline{\underline{D}}_{\hat{k}_{n(t)}} = \mathrm{sym}\left({}^{\xi_i}\underline{\underline{L}}_{\hat{k}_{n(t)}} \right), \tag{18} $$

and the extensive thermodynamic Helmholtz potential (Ψ) can be represented as

$$ \Psi = \Psi\left(\lambda_\nu, \mathcal{I}^{\nu}_{1}, \mathcal{II}^{\nu}_{1}, \mathcal{III}^{\nu}_{1}, ..., \mathcal{I}^{\nu}_{r_\nu}, \mathcal{II}^{\nu}_{r_\nu}, \mathcal{III}^{\nu}_{r_\nu}, \lambda_\mu, \mathcal{I}^{\mu}_{1}, \mathcal{II}^{\mu}_{1}, \mathcal{III}^{\mu}_{1}, ..., \mathcal{I}^{\mu}_{r_\mu}, \mathcal{II}^{\mu}_{r_\mu}, \mathcal{III}^{\mu}_{r_\mu} \right); \tag{19} $$

$$ \therefore \dot{\Psi} = \sum_{i=\nu,\,\mu} \left[\Psi_{,\,\lambda_i} \dot{\lambda}_i + \sum_{\xi_i=1}^{r_i} \left(\Psi_{,\,{}^{\xi_i}\underline{\underline{B}}_{\hat{k}_{n(t)}}} : {}^{\xi_i}\dot{\underline{\underline{B}}}_{\hat{k}_{n(t)}} \right) \right], \tag{20} $$

where follows from chain rule $\underline{\underline{\Psi}}_{,\,{}^{\xi_i}\underline{\underline{B}}_{\hat{k}_{n(t)}}} = \left(\Psi_{,\,\mathcal{I}^{i}_{\xi_i}} + \mathcal{I}^{i}_{\xi_i} \Psi_{,\,\mathcal{II}^{i}_{\xi_i}} \right) \underline{\underline{I}} - \Psi_{,\,\mathcal{II}^{i}_{\xi_i}} \, {}^{\xi_i}\underline{\underline{B}}_{\hat{k}_{n(t)}} + \mathcal{III}^{i}_{\xi_i} \Psi_{,\,\mathcal{III}^{i}_{\xi_i}} \, {}^{\xi_i}\underline{\underline{B}}^{-T}_{\hat{k}_{n(t)}}$, with $\mathcal{I}^{i}_{\xi_i} = tr\left({}^{\xi_i}\underline{\underline{B}}_{\hat{k}_{n(t)}} \right)$, $\mathcal{II}^{i}_{\xi_i} = \frac{1}{2}\left[tr\left({}^{\xi_i}\underline{\underline{B}}_{\hat{k}_{n(t)}} \right)^2 - tr\left({}^{\xi_i}\underline{\underline{B}}^{2}_{\hat{k}_{n(t)}} \right) \right]$ and $\mathcal{III}_{\xi_i} = det\left({}^{\xi_i}\underline{\underline{B}}_{\hat{k}_{n(t)}} \right)$. Without loss of generality it is chosen $\hat{k}_{n(t)}$ such that ${}^{\xi_i}\underline{\underline{F}}_{\hat{k}_{n(t)}} = {}^{\xi_i}\underline{\underline{V}}_{\hat{k}_{n(t)}}$ ($\therefore {}^{\xi_i}\underline{\underline{C}}_{\hat{k}_{n(t)}} = {}^{\xi_i}\underline{\underline{B}}_{\hat{k}_{n(t)}}$), that is, for an appropriate rotated natural configuration $\hat{k}_{n(t)}$, it follows [8]:

$$ \underline{\underline{I}} : {}^{\xi_i}\dot{\underline{\underline{B}}}_{\hat{k}_{n(t)}} = 2 \, {}^{\xi_i}\underline{\underline{B}}_{\hat{k}_{n(t)}} : \left(\underline{\underline{D}} - {}^{\xi_i}\underline{\underline{D}}_{\hat{k}_{n(t)}} \right); \tag{21} $$

$$ {}^{\xi_i}\underline{\underline{B}}_{\hat{k}_{n(t)}} : {}^{\xi_i}\dot{\underline{\underline{B}}}_{\hat{k}_{n(t)}} = 2 \, {}^{\xi_i}\underline{\underline{B}}^{2}_{\hat{k}_{n(t)}} : \left(\underline{\underline{D}} - {}^{\xi_i}\underline{\underline{D}}_{\hat{k}_{n(t)}} \right); \tag{22} $$

$$ {}^{\xi_i}\underline{\underline{B}}^{-T}_{\hat{k}_{n(t)}} : {}^{\xi_i}\dot{\underline{\underline{B}}}_{\hat{k}_{n(t)}} = 2\underline{\underline{I}} : \left(\underline{\underline{D}} - {}^{\xi_i}\underline{\underline{D}}_{\hat{k}_{n(t)}} \right), \tag{23} $$

where $\underline{\underline{D}}$ is the symmetric part of velocity gradient ($\underline{\underline{L}}$). Returning to Eq. (20), one has

$$ \begin{aligned} \dot{\Psi} = \sum_{i=\nu,\,\mu} \Bigg\{ \Psi_{,\,\lambda_i} \dot{\lambda}_i + \sum_{\xi_i=1}^{r_i} 2 \Bigg[& \left(\Psi_{,\,\mathcal{I}_{\xi_i}} + \mathcal{I}^{i}_{\xi_i} \Psi_{,\,\mathcal{II}^{i}_{\xi_i}} \right) {}^{\xi_i}\underline{\underline{B}}_{\hat{k}_{n(t)}} - \Psi_{,\,\mathcal{II}^{i}_{\xi_i}} \, {}^{\xi_i}\underline{\underline{B}}^{2}_{\hat{k}_{n(t)}} \\ & + \mathcal{III}^{i}_{\xi_i} \Psi_{,\,\mathcal{III}^{i}_{\xi_i}} \underline{\underline{I}} \Bigg] : \left(\underline{\underline{D}} - {}^{\xi_i}\underline{\underline{D}}_{\hat{k}_{n(t)}} \right) \Bigg\}. \end{aligned} \tag{24} $$

Then, from the Clausius-Duhem inequality follows the specific rate of dissipation Ξ

$$\begin{aligned}\Xi &= \underline{\underline{\tau}} : \underline{\underline{D}} - \dot{\Psi} \\ &= \left\{ \underline{\underline{\tau}} - \sum_{i=\nu,\,\mu} \sum_{\xi_i=1}^{r_i} 2\left[\left(\Psi,_{\mathcal{I}^i_{\xi_i}} + \mathcal{I}^i_{\xi_i} \Psi,_{\mathcal{II}^i_{\xi_i}} \right)^{\xi_i} \underline{\underline{B}}_{\hat{k}_{n(t)}} - \Psi,_{\mathcal{II}^i_{\xi_i}}{}^{\xi_i} \underline{\underline{B}}^2_{\hat{k}_{n(t)}} + \mathcal{III}^i_{\xi_i} \Psi,_{\mathcal{III}^i_{\xi_i}} \underline{\underline{I}} \right] \right\} \\ &: \underline{\underline{D}} - \sum_{i=\nu,\,\mu} \Psi,_{\lambda_i} \dot{\lambda}_i + \sum_{i=\nu,\,\mu} \sum_{\xi_i=1}^{r_i} 2\left[\left(\Psi,_{\mathcal{I}^i_{\xi_i}} + \mathcal{I}^i_{\xi_i} \Psi,_{\mathcal{II}^i_{\xi_i}} \right)^{\xi_i} \underline{\underline{B}}_{\hat{k}_{n(t)}} - \Psi,_{\mathcal{II}^i_{\xi_i}}{}^{\xi_i} \underline{\underline{B}}^2_{\hat{k}_{n(t)}} \right. \\ &\left. + \mathcal{III}^i_{\xi_i} \Psi,_{\mathcal{III}^i_{\xi_i}} \underline{\underline{I}} \right] :^{\xi_i} \underline{\underline{D}}_{\hat{k}_{n(t)}},\end{aligned} \tag{25}$$

where $\underline{\underline{\tau}}$ is the Cauchy stress tensor.

This approach makes possible the analysis of the constitutive law and the nonnegativity of the entropy production in the context of irreversible thermodynamic processes. In this sense, it is assumed that total rate dissipation Ξ can be divided into three parts, each one associated to a specific process, as follows:

$$\Xi_{\hat{k}_t} = \left\{ \underline{\underline{\tau}} - \sum_{i=\nu,\,\mu} \sum_{\xi_i=1}^{r_i} 2\left[\left(\Psi,_{\mathcal{I}^i_{\xi_i}} + \mathcal{I}^i_{\xi_i} \Psi,_{\mathcal{II}^i_{\xi_i}} \right)^{\xi_i} \underline{\underline{B}}_{\hat{k}_{n(t)}} - \Psi,_{\mathcal{II}^i_{\xi_i}}{}^{\xi_i} \underline{\underline{B}}^2_{\hat{k}_{n(t)}} + \mathcal{III}^i_{\xi_i} \Psi,_{\mathcal{III}^i_{\xi_i}} \underline{\underline{I}} \right] \right\} : \underline{\underline{D}} \geq 0; \tag{26}$$

$$\Xi_{\lambda} = - \sum_{i=\nu,\,\mu} \Psi,_{\lambda_i} \dot{\lambda}_i \geq 0; \tag{27}$$

$$\Xi_{\hat{k}_{n(t)}} = \sum_{i=\nu,\,\mu} \sum_{\xi_i=1}^{r_i} 2\left[\left(\Psi,_{\mathcal{I}^i_{\xi_i}} + \mathcal{I}^i_{\xi_i} \Psi,_{\mathcal{II}^i_{\xi_i}} \right)^{\xi_i} \underline{\underline{B}}_{\hat{k}_{n(t)}} - \Psi,_{\mathcal{II}^i_{\xi_i}}{}^{\xi_i} \underline{\underline{B}}_{\hat{k}_{n(t)}}{}^2 + \mathcal{III}^i_{\xi_i} \Psi,_{\mathcal{III}^i_{\xi_i}} \underline{\underline{I}} \right] :^{\xi_i} \underline{\underline{D}}_{\hat{k}_{n(t)}} \geq 0, \tag{28}$$

where $\Xi_{\hat{k}_t}$ is the dissipation rate due to changes in $\hat{k}_t(\mathcal{B})$), Ξ_{λ} is the dissipation rate due to changes in micro-structure and $\Xi_{\hat{k}_{n(t)}}$ is the dissipation rate due to changes in $\hat{k}_{n(t)}(\mathcal{B})$.

Following similar steps to the work [8], one has

$$\underline{\underline{\tau}} = \sum_{i=\nu,\,\mu} \sum\nolimits_{\xi_i=1}^{r_i} {}^{\xi_i}\underline{\underline{\tau}}, \tag{29}$$

where

$${}^{\xi_i}\underline{\underline{\tau}} = \sum_{i=\nu,\,\mu} \sum_{\xi_i=1}^{r_i} 2\left[\left(\Psi,_{\mathcal{I}^i_{\xi_i}} + \mathcal{I}^i_{\xi_i} \Psi,_{\mathcal{II}^i_{\xi_i}} \right)^{\xi_i} \underline{\underline{B}}_{\hat{k}_{n(t)}} - \Psi,_{\mathcal{II}^i_{\xi_i}}{}^{\xi_i} \underline{\underline{B}}^2_{\hat{k}_{n(t)}} + \mathcal{III}^i_{\xi_i} \Psi,_{\mathcal{III}^i_{\xi_i}} \underline{\underline{I}} \right]. \tag{30}$$

Thus, one has for each ξ_i-relaxation mechanism.

$$\frac{\eta'_{\xi_i}}{G'_{\xi_i}} {}^{\xi_i}\overset{\odot}{\underline{\underline{\tau}}} + \left[1 - \frac{\eta'_{\xi_i} \dot{G}'_{\xi_i}}{G'^2_{\xi_i}} \right]^{\xi_i} \underline{\underline{\tau}} = \eta'_{\xi_i} \underline{\underline{D}}, \tag{31}$$

where $\overset{\odot}{()} = \dot{()} - \underline{\underline{L}}() - ()\underline{\underline{L}}^T$ is the "Oldroyd time derivative". Considering the two relaxation mechanisms, with $r_\nu = r_\mu = 1 \therefore {}^{\xi_\nu}\underline{\underline{\tau}} = \underline{\underline{\tau}}_\nu$ and ${}^{\xi_\mu}\underline{\underline{\tau}} = \underline{\underline{\tau}}_\mu$, where $\eta'_{\xi_\nu} = \eta_\nu$, $G'_{\xi_\nu} = G$, $\eta'_{\xi_\mu} = \eta_\mu$ and $G'_{\xi_\mu} \to +\infty$, one has.

$$\frac{\eta_\nu}{G}\overset{\odot}{\underline{\underline{\tau}}}_\nu + \left[1 - \frac{\eta_\nu \dot{G}}{G^2}\right]\underline{\underline{\tau}}_\nu = \eta_\nu \underline{\underline{D}}; \tag{32}$$

$$\underline{\underline{\tau}}_\mu = \eta_\mu \underline{\underline{D}}. \tag{33}$$

Therefore, as $\underline{\underline{\tau}} = \underline{\underline{\tau}}_\nu + \underline{\underline{\tau}}_\mu$ one has

$$\frac{\eta_\nu}{G}\overset{\odot}{\underline{\underline{\tau}}} + \left(1 - \frac{\eta_\nu \dot{G}}{G^2}\right)\underline{\underline{\tau}} = \left[\eta_\nu + \left(1 - \frac{\eta_\nu \dot{G}}{G^2}\right)\eta_\mu + \frac{\eta_\nu \dot{\eta}_\mu}{G}\right]\underline{\underline{D}} + \frac{\eta_\nu \eta_\mu}{G}\overset{\odot}{\underline{\underline{D}}}. \tag{34}$$

Note that the isochoric motion constraint was not required in this analysis. In this way, associating each relaxation mechanism to a micro-structure, it is important to point out that depending on the nature (level of complexity) of the analyzed thixotropic substance, the reasoning presented here can be extrapolated for more than two relaxation mechanisms (i.e., more than two micro-structure types) aiming a consistent/coherent (in thermodynamic and rheological senses) approach of the model.

4. On the transition region

The objective of this topic is to analyze the transition/yielding region criteria under a theoretical and formal point of view. In this sense, it is important to stand out that the constitutive equation

$$\frac{\eta_\nu}{G}\overset{\odot}{\underline{\underline{\tau}}} + \left(1 - \frac{\eta_\nu \dot{G}}{G^2}\right)\underline{\underline{\tau}} = \left[\eta_\nu + \left(1 - \frac{\eta_\nu \dot{G}}{G^2}\right)\eta_\mu + \frac{\eta_\nu \dot{\eta}_\mu}{G}\right]\underline{\underline{D}} + \frac{\eta_\nu \eta_\mu}{G}\overset{\odot}{\underline{\underline{D}}}, \tag{35}$$

can be rewritten in a more appropriate form as follows:

$$\theta_1 \overset{\odot}{\underline{\underline{\Pi}}} + \underline{\underline{\Pi}} = \eta\left(\dot{\underline{\underline{\Gamma}}} + \theta_2 \overset{\odot}{\dot{\underline{\underline{\Gamma}}}}\right), \tag{36}$$

where

$$\underline{\underline{\Pi}} = \frac{\underline{\underline{\tau}}}{G}; \tag{37}$$

$$\dot{\underline{\underline{\Gamma}}} = \frac{\eta_\mu}{G}\underline{\underline{D}}; \tag{38}$$

$$\eta = \frac{\eta_\nu + \eta_\mu}{\eta_\mu}; \tag{39}$$

$$\theta_1 = \frac{\eta_\nu}{G}; \tag{40}$$

$$\theta_2 = \frac{\eta_\nu \eta_\mu}{G\left(\eta_\nu + \eta_\mu\right)}. \tag{41}$$

It can be seen that the form of Eq. (36) is quite similar to the standard Jeffreys model. The quantities Π, $\dot{\Gamma}$, η, θ_1 and θ_2 can be interpreted as a dimensionless stress, dimensionless strain, dimensionless apparent viscosity, relaxation time and retardation time, respectively. Note that since

$$\dot{\overline{G^{-1}}} = \left(G^{-1}\right)_{,\lambda_\nu}\dot{\lambda}_\nu \to 0;$$

$$\dot{\overline{\frac{\eta_\mu}{G}}} = \left(\frac{\eta_\mu}{G}\right)_{,\lambda_\mu}\dot{\lambda}_\mu + \left(\frac{\eta_\mu}{G}\right)_{,\lambda_\nu}\dot{\lambda}_\nu \to 0,$$

Eq. (36) corresponds to the standard Jeffreys model. In this way, it is clear the relation between the nonlinear viscoelastic region (associated to the thixotropic effect) and $\dot{\lambda}$. Many works propose that an indicative for the beginning of the transition/yielding region is a region where occurs the modification in the behavior of the thixotropic substance, from the linear viscoelastic region to nonlinear viscoelastic region [37–41] associating an specific strain value for that. However, this specific value is not constant [41–45].

In this sense, taking into account the mapping in terms of variables in the actual configurations ($\underline{x} = x^i\underline{g}_i$) and the respective displacements ($\underline{u} = u^i\underline{g}_i$), it follows:

$$\begin{bmatrix} \frac{\partial(x^1-u^1)}{\partial x^1} & \frac{\partial(x^2-u^2)}{\partial x^1} & \frac{\partial(x^3-u^3)}{\partial x^1} \\ \frac{\partial(x^1-u^1)}{\partial x^2} & \frac{\partial(x^2-u^2)}{\partial x^2} & \frac{\partial(x^3-u^3)}{\partial x^2} \\ \frac{\partial(x^1-u^1)}{\partial x^3} & \frac{\partial(x^2-u^2)}{\partial x^3} & \frac{\partial(x^3-u^3)}{\partial x^3} \end{bmatrix} = \begin{bmatrix} 1-\frac{\partial u^1}{\partial x^1} & -\frac{\partial u^2}{\partial x^1} & -\frac{\partial u^3}{\partial x^1} \\ -\frac{\partial u^1}{\partial x^2} & 1-\frac{\partial u^2}{\partial x^2} & -\frac{\partial u^3}{\partial x^2} \\ -\frac{\partial u^1}{\partial x^3} & -\frac{\partial u^2}{\partial x^3} & 1-\frac{\partial u^3}{\partial x^3} \end{bmatrix},$$

and in this context, one has the Jacobian ($\tilde{J}$)

$$\tilde{J} = \det\begin{pmatrix} 1-\frac{\partial u^1}{\partial x^1} & -\frac{\partial u^2}{\partial x^1} & -\frac{\partial u^3}{\partial x^1} \\ -\frac{\partial u^1}{\partial x^2} & 1-\frac{\partial u^2}{\partial x^2} & -\frac{\partial u^3}{\partial x^2} \\ -\frac{\partial u^1}{\partial x^3} & -\frac{\partial u^2}{\partial x^3} & 1-\frac{\partial u^3}{\partial x^3} \end{pmatrix}, \tag{42}$$

and

$$\begin{aligned} \tilde{J}^2 &= \det\begin{pmatrix} 1-2\varepsilon_{11} & -2\varepsilon_{12} & -2\varepsilon_{13} \\ -2\varepsilon_{21} & 1-2\varepsilon_{22} & -2\varepsilon_{23} \\ -2\varepsilon_{31} & -2\varepsilon_{32} & 1-2\varepsilon_{33} \end{pmatrix}; \\ &= 8(\varepsilon_{11}\varepsilon_{23}\varepsilon_{32} + \varepsilon_{12}\varepsilon_{21}\varepsilon_{33} + \varepsilon_{13}\varepsilon_{22}\varepsilon_{31} - \varepsilon_{11}\varepsilon_{22}\varepsilon_{33} - \varepsilon_{12}\varepsilon_{23}\varepsilon_{31} - \varepsilon_{13}\varepsilon_{32}\varepsilon_{21}) \\ &\quad +4(\varepsilon_{11}\varepsilon_{33} + \varepsilon_{11}\varepsilon_{22} + \varepsilon_{22}\varepsilon_{33} - \varepsilon_{12}\varepsilon_{21} - \varepsilon_{13}\varepsilon_{31} - \varepsilon_{23}\varepsilon_{32}) \\ &\quad -2(\varepsilon_{11} + \varepsilon_{22} + \varepsilon_{33}) + 1; \\ &= -8\mathcal{J}\mathcal{J}\mathcal{J} + 4\mathcal{J}\mathcal{J} - 2\mathcal{J} + 1, \end{aligned} \tag{43}$$

with

$$2\varepsilon_{ij} = \begin{cases} 2\frac{\partial u^j}{\partial x^i} - \left(\frac{\partial u^1}{\partial x^i}\right)^2 - \left(\frac{\partial u^2}{\partial x^i}\right)^2 - \left(\frac{\partial u^3}{\partial x^i}\right)^2, & \text{if } i = j; \\ \left(\frac{\partial u^j}{\partial x^i} + \frac{\partial u^i}{\partial x^j}\right) - \frac{\partial u^1}{\partial x^i}\frac{\partial u^1}{\partial x^j} - \frac{\partial u^2}{\partial x^i}\frac{\partial u^2}{\partial x^j} - \frac{\partial u^3}{\partial x^i}\frac{\partial u^3}{\partial x^j}, & \text{if } i \neq j; \end{cases}$$

and

$$\mathcal{J} = \frac{1}{1!}\delta^{i}_{j}\varepsilon^{j}_{i}; \tag{44}$$

$$\mathcal{J}\mathcal{J} = \frac{1}{2!}\delta^{ij}_{kl}\varepsilon^{l}_{j}\varepsilon^{k}_{i}; \tag{45}$$

$$\mathcal{J}\mathcal{J}\mathcal{J} = \frac{1}{3!}\delta^{ijk}_{rst}\varepsilon^{t}_{k}\varepsilon^{s}_{j}\varepsilon^{r}_{i}, \tag{46}$$

where δ^{ij}_{kl} and δ^{ijk}_{rst} are the generalized Kronecker delta [46, 47]. Thus, the relationship between dV (differential of volume in the reference configuration) and dv (differential of volume in the actual configuration) can be described in the following way:

$$dV = (-8\mathcal{J}\mathcal{J}\mathcal{J} + 4\mathcal{J}\mathcal{J} - 2\mathcal{J} + 1)^{\frac{1}{2}}dv. \tag{47}$$

Taking into account that the yield region can be characterized as a transition region. This region, in fact, can be treated as a singularity region. As the continuity axiom holds a suitable asymptotic behavior [48–50], the concept of transition phenomenon has an asymptotic nature, and can be treated by limiting approaches. Physically, the transition region (transition/yielding) can be noted when a substance loses part of their original intrinsic properties, and from this point a new set of properties are raised in this substance, resulting in a new behavior. For example, in an elasto-plastic transition behavior, the transition state is related to a strain ellipsoid degeneracy, in a geometric sense, which can be transformed to an infinite cylinder, point or a pair of planes [51].

Considering the abovementioned lines, it can be imagined the nonlinear viscoelastic region as a direct mapping image from the linear viscoelastic region. Thus, the Jacobian $(\tilde{J})$, of this mapping, should translate the singularity on the transition region vicinity as an asymptotic extremely large deformation of the original microscopic element. In other words, taking into account Eq. (47), it can be seen that for a finite initial volume dV, with $\tilde{J} \to 0$ (singularity on the neighbor of the transition region) implicates in $dv \to \infty$, and in this way, it can write for the transition region the following condition:

$$8\mathcal{J}\mathcal{J}\mathcal{J} - 4\mathcal{J}\mathcal{J} + 2\mathcal{J} = 1, \tag{48}$$

or in an asymptotic sense on the transition region (t.r.)

$$\lim_{\underline{\underline{\varepsilon}} \to \text{t.r.}} (8\mathcal{J}\mathcal{J}\mathcal{J} - 4\mathcal{J}\mathcal{J} + 2\mathcal{J}) = 1. \tag{49}$$

It is important to stand out that this condition was stated in terms of the strain invariants, which can be rewritten in terms of the stress invariants or in terms of energy, by the constitutive relationships. Note the difficulty involved in expressing the strain tensor invariants in terms of the stress tensor invariants, due to the constitutive model's form.

Remark 1. *If it is taken the time rate of* Eq. (48), *one has*

$$4\dot{\overline{\mathcal{J}\mathcal{J}\mathcal{J}}} - 2\dot{\overline{\mathcal{J}\mathcal{J}}} + \dot{\mathcal{J}} = 0;$$

$$\therefore 4\mathcal{J}\mathcal{J}\mathcal{J}\underline{\underline{\varepsilon}}^{-T} : \underline{\underline{\dot{\varepsilon}}} - 2\left[\mathcal{J}\mathcal{J}tr\left(\underline{\underline{\dot{\varepsilon}}}\right) - \underline{\underline{\varepsilon}} : \underline{\underline{\dot{\varepsilon}}}\right] + tr\left(\underline{\underline{\dot{\varepsilon}}}\right) = 0;$$

or

$$4\mathcal{J}\mathcal{J}\mathcal{J}\underline{\underline{\varepsilon}}^{-T} : \underline{\underline{D}} - 2\left[\mathcal{J}\mathcal{J}tr\left(\underline{\underline{D}}\right) - \underline{\underline{\varepsilon}} : \underline{\underline{D}}\right] + tr\left(\underline{\underline{D}}\right) = 0. \tag{50}$$

Supposing the case that the strain rate is obtained as a response to known stress load, returning to Eq. (36), it follows:

$$\overset{\odot}{\underline{\underline{\Pi}}} + \theta_1^{-1}\underline{\underline{\Pi}} = \frac{G(\eta_\nu + \eta_\mu)}{\eta_\nu \eta_\mu}\dot{\underline{\underline{\Gamma}}} + \overset{\odot}{\dot{\underline{\underline{\Gamma}}}}, \tag{51}$$

or

$$\overset{\odot}{\dot{\underline{\underline{\Gamma}}}} + \phi'\dot{\underline{\underline{\Gamma}}} = \underline{\underline{\psi}}', \tag{52}$$

with

$$\underline{\underline{\psi}}' = \overset{\odot}{\underline{\underline{\Pi}}} + \theta_1^{-1}\underline{\underline{\Pi}};$$

$$\phi' = \frac{G(\eta_\nu + \eta_\mu)}{\eta_\mu \eta_\nu}.$$

Thus, one has

$$\vartheta'\overset{\odot}{\dot{\underline{\underline{\Gamma}}}} + \vartheta'\phi'\dot{\underline{\underline{\Gamma}}} = \overset{\odot}{\overline{\vartheta'\dot{\underline{\underline{\Gamma}}}}} = \vartheta'\underline{\underline{\psi}}' \therefore \overset{\odot}{\underline{\underline{\Theta}}} = \underline{\underline{\psi}}, \tag{53}$$

where

$$\vartheta'(t) = exp\left(\int \phi' dt\right);$$

$$\underline{\underline{\psi}}(t) = \vartheta'\underline{\underline{\psi}}';$$

$$\underline{\underline{\Theta}} = \vartheta'\dot{\underline{\underline{\Gamma}}}.$$

Note that

$$\overline{\underline{\underline{F}}\left(\underline{\underline{F}}^{-1}\underline{\underline{\Theta}}\underline{\underline{F}}^{-T}\right)\underline{\underline{F}}^{T}} = \dot{\underline{\underline{F}}}\left(\underline{\underline{F}}^{-1}\underline{\underline{\Theta}}\underline{\underline{F}}^{-T}\right)\underline{\underline{F}}^{T} + \underline{\underline{F}}\overline{\left(\underline{\underline{F}}^{-1}\underline{\underline{\Theta}}\underline{\underline{F}}^{-T}\right)}\underline{\underline{F}}^{T} + \dot{\underline{\underline{F}}}\left(\underline{\underline{F}}^{-1}\underline{\underline{\Theta}}\underline{\underline{F}}^{-T}\right)\dot{\underline{\underline{F}}}^{T};$$

$$\therefore \dot{\underline{\underline{\Theta}}} = \underline{\underline{L}}\underline{\underline{\Theta}} + \underline{\underline{F}}\overline{\left(\underline{\underline{F}}^{-1}\underline{\underline{\Theta}}\underline{\underline{F}}^{-T}\right)}\underline{\underline{F}}^{T} + \underline{\underline{\Theta}}\underline{\underline{L}}^{T};$$

$$\therefore \dot{\underline{\underline{\Theta}}} - \underline{\underline{L}}\underline{\underline{\Theta}} - \underline{\underline{\Theta}}\underline{\underline{L}}^{T} = \underline{\underline{F}}\overline{\left(\underline{\underline{F}}^{-1}\underline{\underline{\Theta}}\underline{\underline{F}}^{-T}\right)}\underline{\underline{F}}^{T}, \tag{54}$$

and in this way, from Eq. (53), it follows:

$$\overset{\odot}{\underline{\underline{\Theta}}} = \underline{\underline{F}}\overline{\left(\underline{\underline{F}}^{-1}\underline{\underline{\Theta}}\underline{\underline{F}}^{-T}\right)}\underline{\underline{F}}^{T} = \underline{\underline{\psi}};$$

$$\therefore \overline{\left(\underline{\underline{F}}^{-1}\underline{\underline{\Theta}}\underline{\underline{F}}^{-T}\right)} = \underline{\underline{F}}^{-1}\underline{\underline{\psi}}\underline{\underline{F}}^{-T};$$

$$\therefore \underline{\underline{\Theta}}(t) = \underline{\underline{F}}(t)\left(\int_0^t \underline{\underline{F}}^{-1}(t')\underline{\underline{\psi}}(t')\underline{\underline{F}}^{-T}(t')\ dt'\right)\underline{\underline{F}}^{T}(t);$$

$$\therefore \dot{\underline{\underline{\Gamma}}}(t) = \frac{1}{\vartheta'(t)}\underline{\underline{F}}(t)\left(\int_0^t \underline{\underline{F}}^{-1}(t')\underline{\underline{\psi}}(t')\underline{\underline{F}}^{-T}(t')\ dt'\right)\underline{\underline{F}}^{T}(t),$$

or in other words

$$\underline{\underline{D}}(t) = \frac{G}{\eta_\mu \vartheta'(t)} \underline{\underline{F}}(t) \left(\int_0^t \underline{\underline{F}}^{-1}(t') \underline{\underline{\psi}}(t') \underline{\underline{F}}^{-T}(t') \; dt' \right) \underline{\underline{F}}^{T}(t);$$

$$= \frac{G}{\eta_\mu \vartheta'(t)} \underline{\underline{F}}(t) \left[\int_0^t \underline{\underline{F}}^{-1}(t') \vartheta'(t') \left(\overset{\odot}{\underline{\underline{\Pi}}}(t') + \theta_1^{-1} \underline{\underline{\Pi}}(t') \right) \underline{\underline{F}}^{-T}(t') \; dt' \right] \underline{\underline{F}}^{T}(t);$$

$$\therefore \underline{\underline{D}}(t) = \frac{G}{\eta_\mu \vartheta'(t)} \underline{\underline{F}}(t) \left\{ \int_0^t \underline{\underline{F}}^{-1}(t') \exp\left(\int \frac{G(\eta_\nu + \eta_\mu)}{\eta_\mu \eta_\nu} dt' \right) \right.$$

$$\left[\dot{\left(\frac{1}{G} \right)} \underline{\underline{\tau}}(t') + G^{-1} \left(\underline{\underline{\tau}}_{,t'}(t') + \underline{\underline{\tau}}(t') \cdot \underline{\underline{\upsilon}}(t') - \underline{\underline{L}}(t') \underline{\underline{\tau}}(t') - \underline{\underline{\tau}}(t') \underline{\underline{L}}^{T}(t') \right) \right.$$

$$\left. \left. + \frac{\underline{\underline{\tau}}(t')}{\eta_\nu} \right] \underline{\underline{F}}^{-T}(t') \; dt' \right\} \underline{\underline{F}}^{T}(t), \tag{55}$$

where $\underline{\underline{L}} = \underline{\upsilon}$ ("Eulerian gradient"), and where $\underline{\upsilon}$ is the velocity field. Consequently,

$$\underline{\underline{\varepsilon}}(t) = \frac{G}{\eta_\mu} \int_0^t \frac{1}{\vartheta'(t')} \underline{\underline{F}}(t') \left\{ \int_0^{t'} \underline{\underline{F}}^{-1}(t'') \exp\left(\frac{G(\eta_\nu + \eta_\mu)}{\eta_\mu \eta_\nu} t'' \right) \right.$$

$$\left[G^{-1} \left(\underline{\underline{\tau}}_{,t''}(t'') + \underline{\underline{\tau}}(t'') \cdot \underline{\underline{\upsilon}}(t'') - \underline{\underline{L}}\left(t''\right) \underline{\underline{\tau}}(t'') - \underline{\underline{\tau}}(t'') \underline{\underline{L}}^{T}(t'') \right) \right.$$

$$\left. \left. + \eta_\nu^{-1} \underline{\underline{\tau}}(t'') \right] \underline{\underline{F}}^{-T}(t'') \; dt'' \right\} \underline{\underline{F}}^{T}(t') dt', \tag{56}$$

since λ_μ and λ_ν are taken as constants (pre-transition/yield region). In this way, the criteria Eq. (48) and/or Eq. (50) can be appropriately analyzed for a stress load excitation.

5. Numerical results

In this section, some illustrative numerical results are presented. Two types of rheological tests are analyzed, the constant shear rate test (CR) and the constant shear stress test (CS). In both cases it is necessary to define consistent initial conditions in relation to physical and mathematical principles. The finite difference method was implemented in MATLAB, with the following set of parameters: $\aleph = 1$, $\eta_0 = 0.08$ Pa.s, $\alpha_1 = 5$, $\alpha_2 = \alpha_3 = 0.5$, $k_\nu \varsigma_\nu = 10^3$ J/m^3, $k_\mu \varsigma_\mu = 10^2$ J/m^3, $\beta_\nu = 5$, $\beta_\mu = 3$, $m = 10^{-6}$, $K_\nu^* = 0.001$ Kg m^{-1}K^{-1}, $K_\mu^* = 0.01$ Kg m^{-1}K^{-1}, $G_0 = 6.5$ Pa, $t_\nu \varsigma_\nu = 10^4$ s^{-1} and $t_\mu \varsigma_\mu = 10^3$ s^{-1}. It is important to point out that for both tests it was used $\Delta t = 10^{-3}$ s. It is also important to comment that time-steps $\Delta t = 10^{-4}$ s, 10^{-5} s and 10^{-6} s were analyzed, but modifications in responses were not noted. The tolerance used for the Newton's method was 10^{-6}. Numerical results for real thixotropic substances (numerical/experimental comparative responses, regularization methods associated to nonlinear identification parameter problem, etc.) can be found in [52].

5.1. Constant shear rate test

In this section, it is considered the constant shear rate test, that is taken into account load conditions as $\dot{\gamma}(t) = H(t)\dot{\gamma}_0$, where $H(t)$ represents the standard Heaviside function and $\dot{\gamma}_0$ it is a positive real constant. It is reasonable to think that in the begin of the test, the micro-structure is in a fully structured state $(\lambda_\mu(0) = \lambda_\nu(0) = 1)$.

Figure 3 shows an interesting aspect, for the loads $\dot{\gamma}_0 = 10^{-2}$ s^{-1} and 10^{-1} s^{-1} the behavior is close to a purely viscoelastic response. These behaviors are in agreement with **Figures 4** and **5**, for the same loads. Note that these two shear rates correspond to a low level of modification in λ_μ and λ_ν. In these both cases, the stress of steady state is the maximum stress reached.

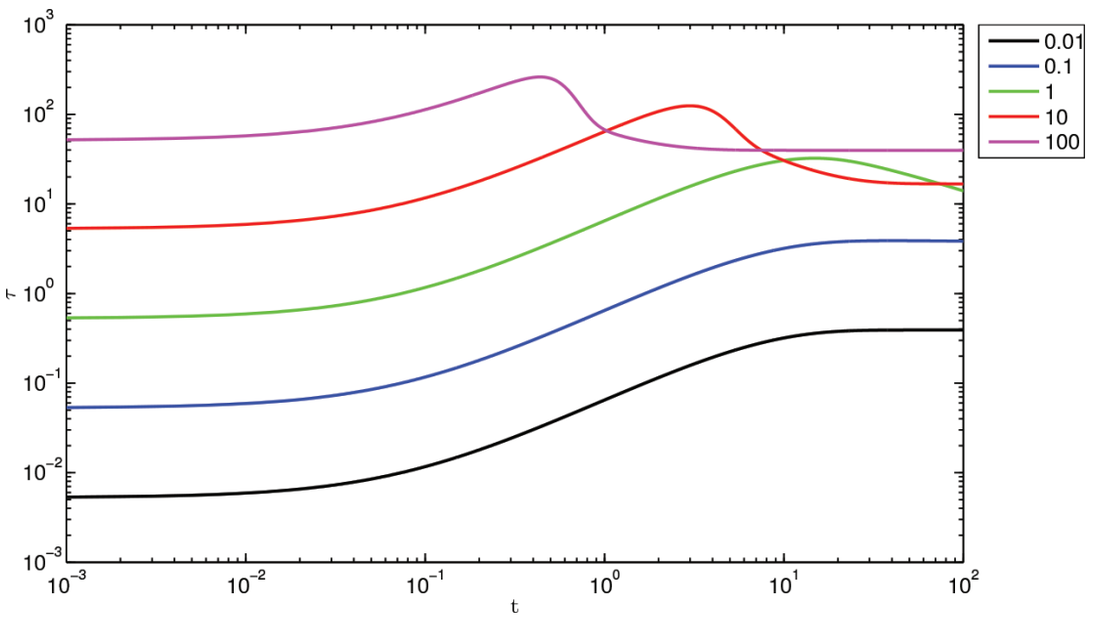

Figure 3.
τ vs. t.

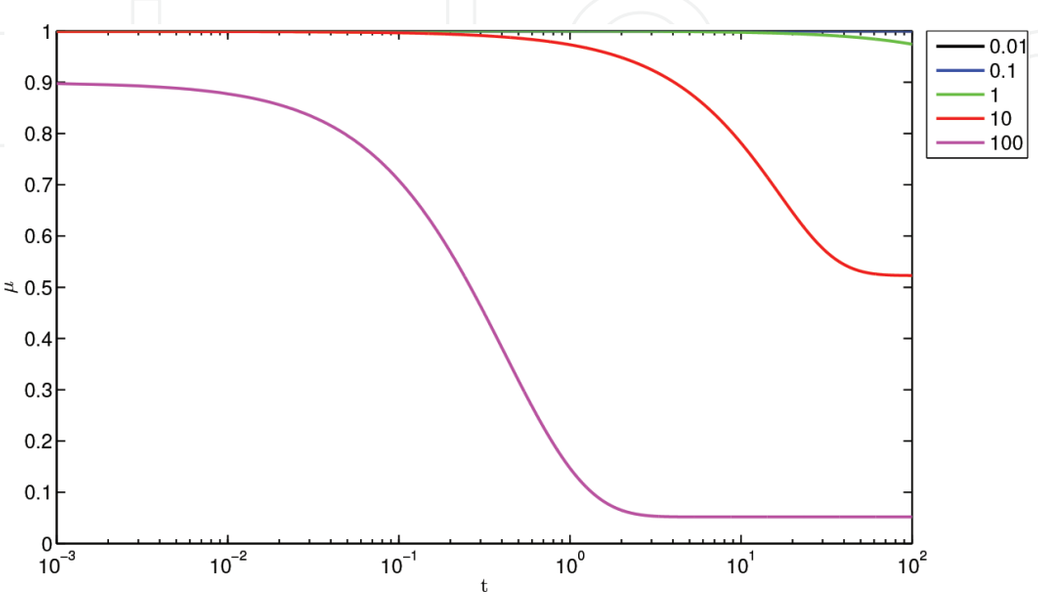

Figure 4.
λ_μ vs. t.

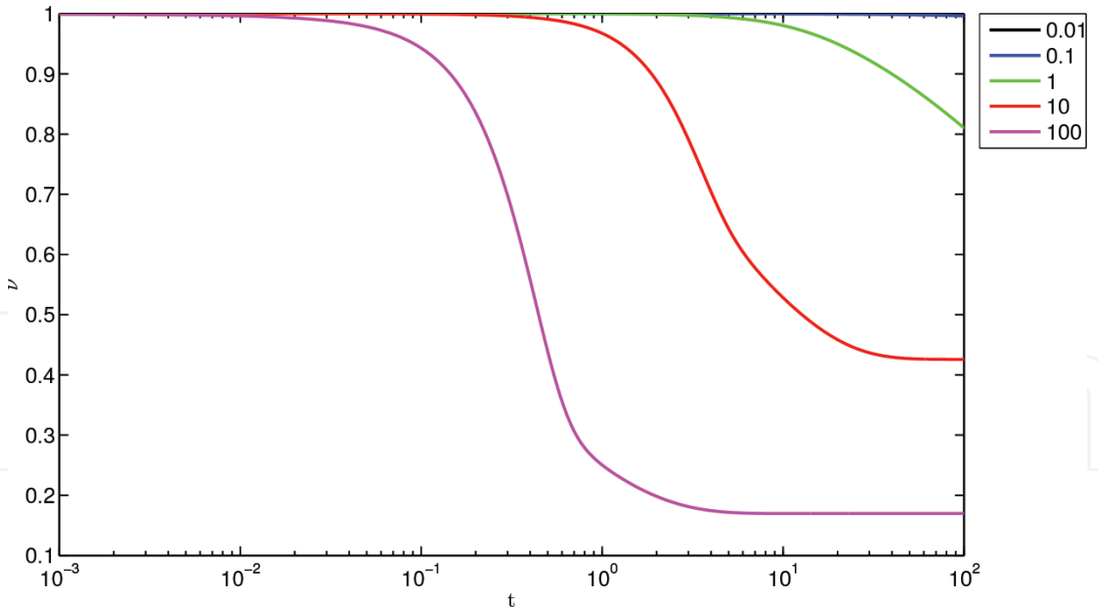

Figure 5.
λ_ν vs. t.

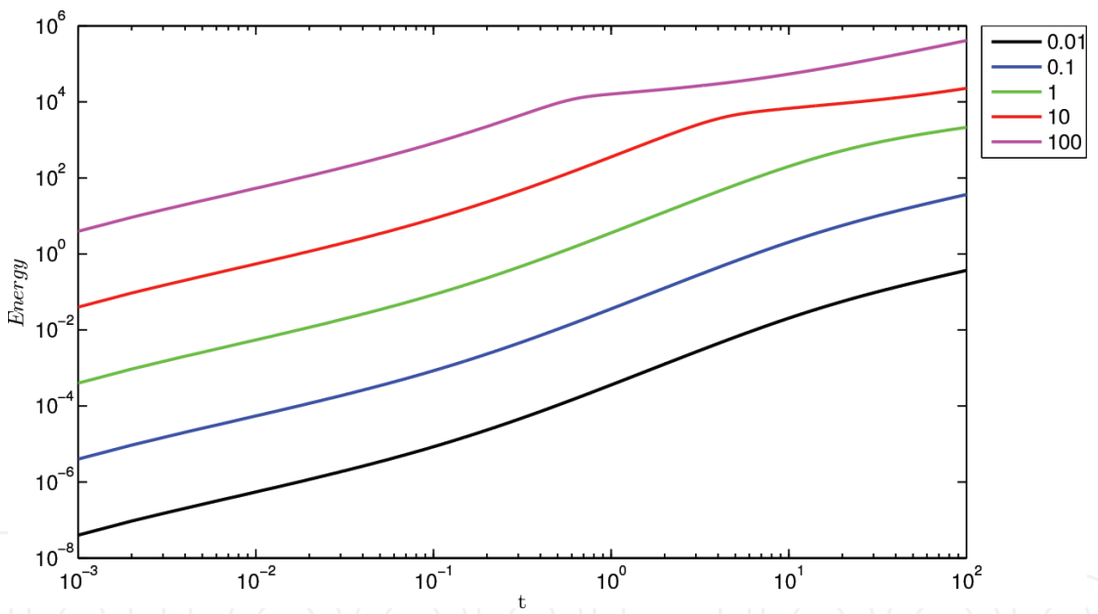

Figure 6.
Energy vs. t.

It is important to point out that for $\dot{\gamma}_0 = 1\ \ s^{-1}$ the thixotropic effect can ever be noted in stress response (**Figure 3**). The loads $\dot{\gamma}_0 = 10\ \ s^{-1}$ and $100\ \ s^{-1}$ show a typical thixotropic behavior (**Figure 3**). These responses are related to considerable modifications in the structural nature of the substance, as can be seen in **Figures 4** and **5**. In these both cases, the maximum stress occurs before the steady state. It can be proved, in a theoretical/mathematical sense, that the point where the maximum breakdown rate occurs is before the stress peak. This fact is in agreement with expected behavior of thixotropic substance.

Other interesting result is related to the energy behavior of the thixotropic substance (**Figures 6** and **7**). Note the presence of a specific slope change in the region where higher rates of decrease on the micro-structures (λ_μ, λ_μ) levels occurred. The same behavior can be observed on experimental results. In fact, this can be explained, in a theoretical sense, via the following relationship

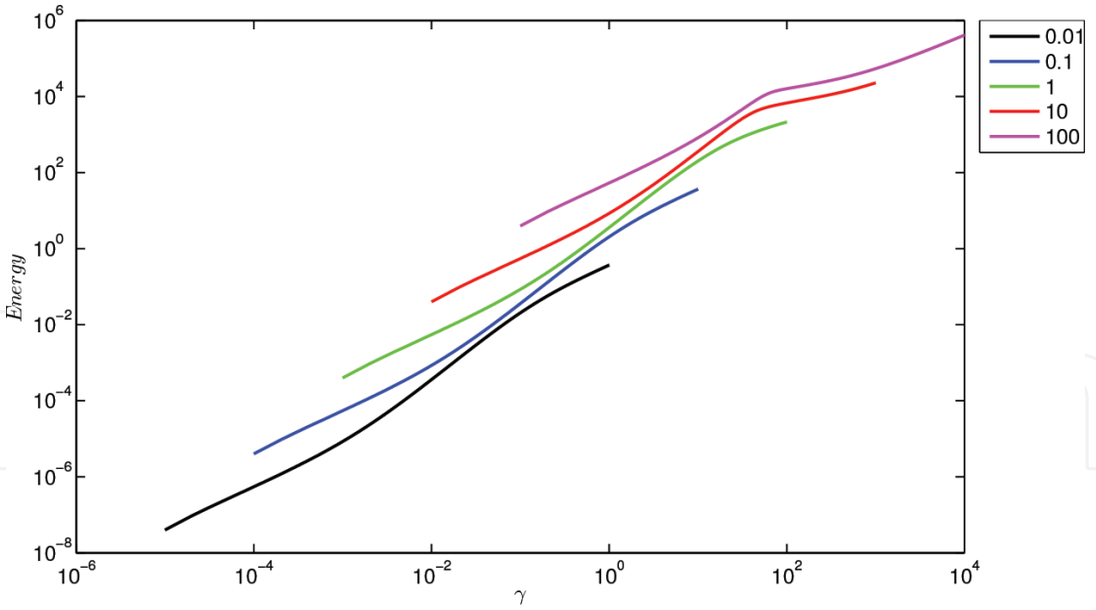

Figure 7.
Energy vs. γ.

$$Power = k_\mu \varsigma_\mu \frac{(1-\lambda_\mu)^\beta}{\lambda_\mu} - t_\mu \varsigma_\mu \frac{\dot{\lambda}_\mu}{\lambda_\mu} + k_\nu \varsigma_\nu \frac{(1-\lambda_\nu)^\beta}{\lambda_\nu} - t_\nu \varsigma_\nu \frac{\dot{\lambda}_\nu}{\lambda_\nu}, \tag{57}$$

that comes from the rate Eqs. (11) and (12).

5.2. Constant stress test

This chapter presents some points and results for the constant shear stress test. In this sense, it is considered loads as $\tau(t) = H(t)\tau_0$, where $H(t)$ represents the standard Heaviside function and τ_0 is a positive real constant. It is assumed that in the begin of the test, the micro-structure is in a fully structured state $(\lambda_\mu(0) = \lambda_\nu(0) = 1)$.

It can be seen in **Figure 8**, for the loads $\tau_0 = 10$, 20, 30, 40, 50 and 100 Pa, a typical behavior for thixotropic substances under low level of constant stress loads.

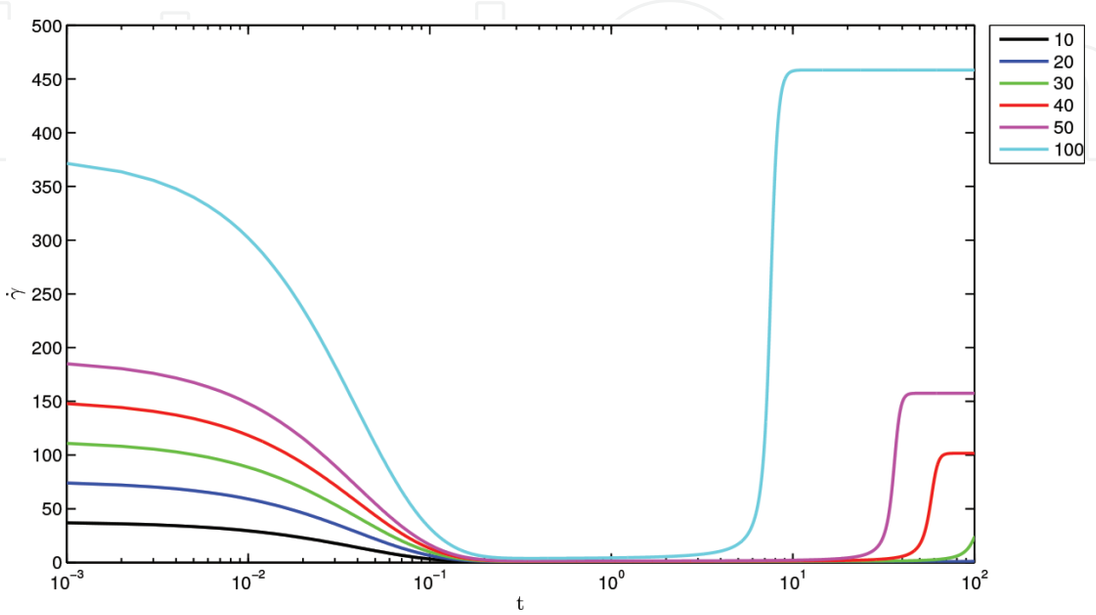

Figure 8.
$\dot{\gamma}$ vs. t.

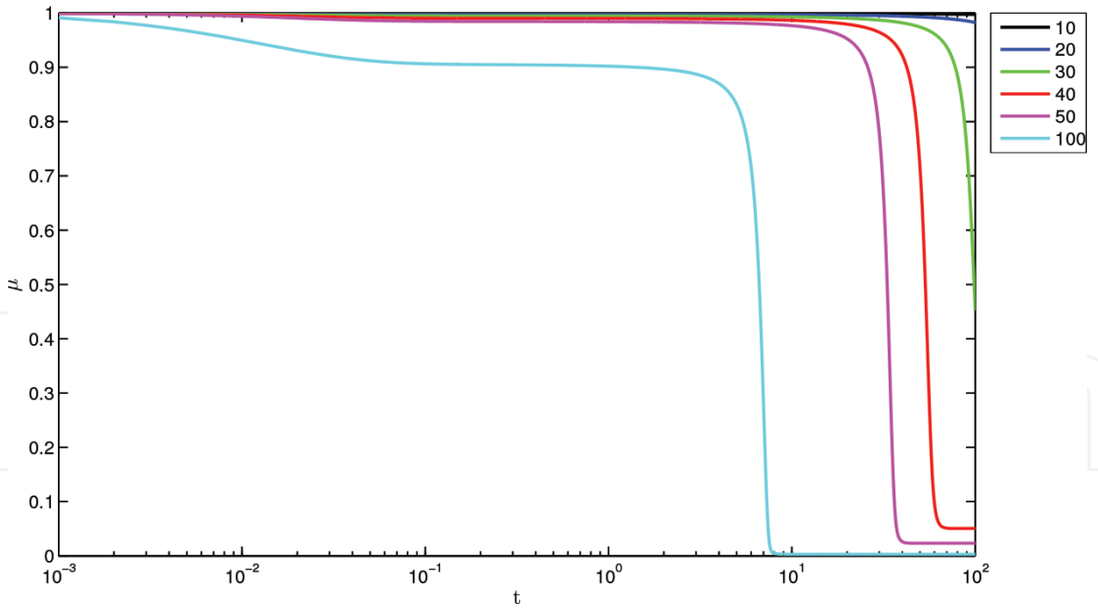

Figure 9.
λ_μ vs. t.

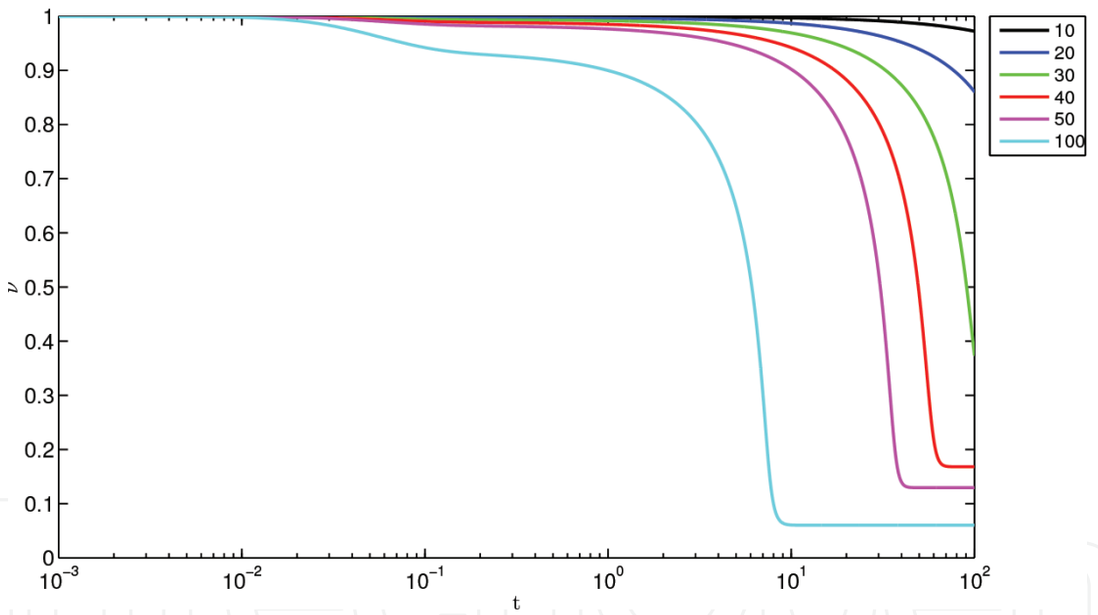

Figure 10.
λ_ν vs. t.

In this test, it can be seen the "Avalanche effect," and their relation with the micro-structural level (λ_μ, λ_ν) of the substance (**Figures 9** and **10**). In these cases, it can be observed the strain rate decrease, related to an increase of the construction parcel (cp_μ) and decrease of the destruction parcel (dp_μ) of λ_μ, as can be seen in **Figures 11** and **12** respectively, where

$$cp_\mu = \frac{1}{t_\mu}\left(k_\mu\left(1-\lambda_\mu\right)^{\beta_\mu}\right); \tag{58}$$

$$dp_\mu = \frac{\left(K_\mu^* \lambda_\mu^6 \theta\ddot{\gamma} + \tau_\mu\right)\lambda_\mu\dot{\gamma}}{\varsigma_\mu}. \tag{59}$$

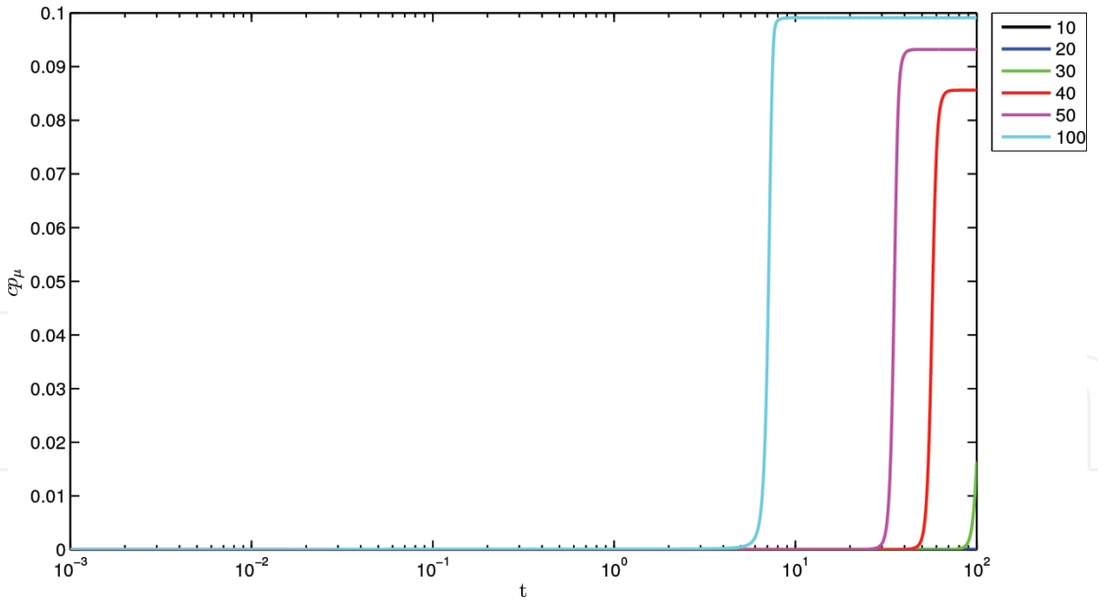

Figure 11.
cp_μ vs. t.

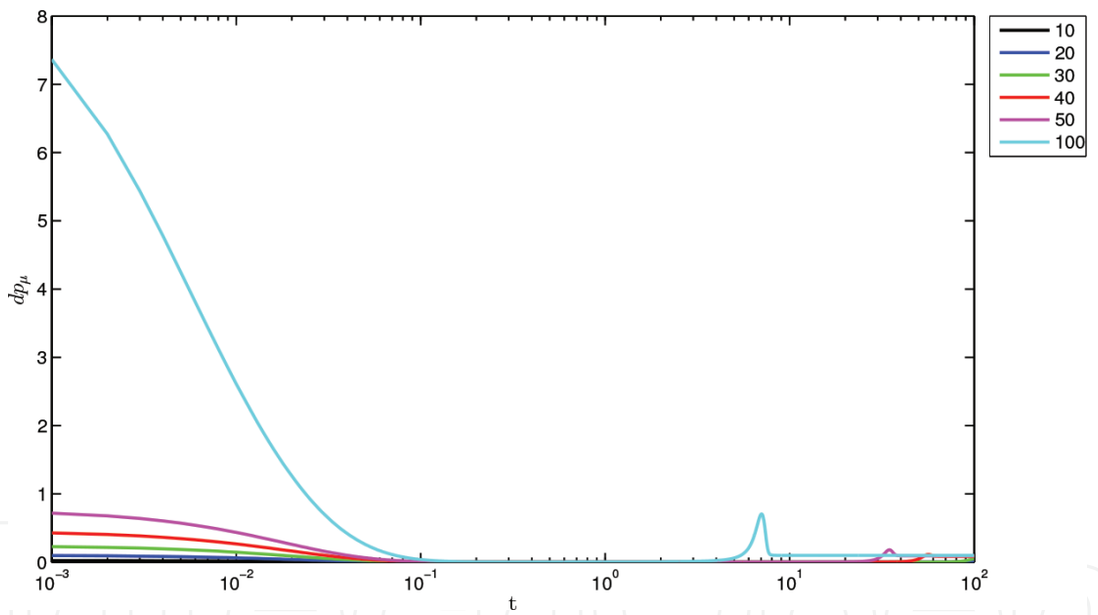

Figure 12.
dp_μ vs. t.

For the Maxwell element ($.\nu$), in the same region (the strain rate decreases), cp_ν is close to null value and dp_ν is increasing, but this increase level is not sufficient to stop the decreasing process of $\dot{\lambda}$. A posterior increase of $\dot{\gamma}$ is due to an abrupt decrease of linkages number (λ_μ, λ_ν) before the steady state.

It is important to note the relationship between the structural nature and the behavior of the substance (**Figures 9** and **10**). Small changes in the values of λ_μ and λ_ν were detected for stress loads 10 and 20 Pa, in relation to the others. In these two cases $\dot{\gamma}$ presents an nonincreasing behavior.

Other interesting result is presented in **Figure 13**, where it can be seen the energy behavior along the test. Note a changing on slope of the energy lines, tending to horizontal slope, in the $\dot{\gamma}$ decreasing region and another one related to the $\dot{\gamma}$ increasing region.

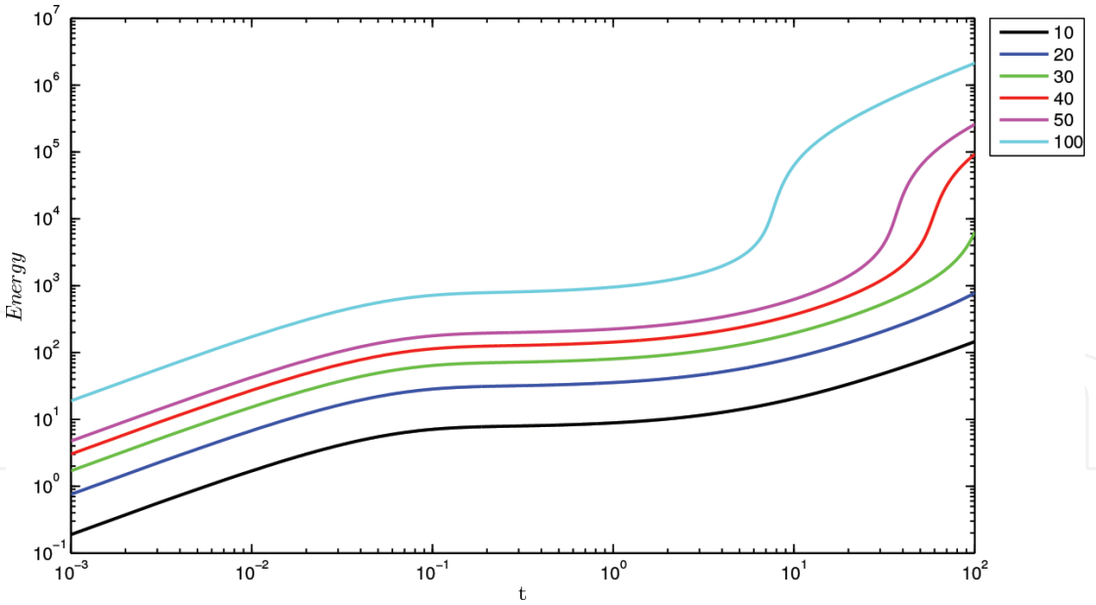

Figure 13.
Energy vs. t.

6. Concluding remarks

The main objective of this chapter is to investigate the constitutive model for thixotropic fluids based on [8] related to the existence of two different types of micro-structure, and their consistence in some rheological tests. The model and analysis presented here are based on well-established physics principles. In this sense, it is important to stand out some nonstandard points of the approach presented in this work for thixotropic modeling in respect to the others models. In this sense, it is important to stand out some points:

- the shear modulus ($G(\lambda_\nu)$), the viscosity coefficients ($\eta_\mu(\lambda_\mu)$ and $\eta_\nu(\lambda_\nu)$) and their dependences from the two different micro-structure types are considered in the development of the constitutive model (Eqs. (9)–(14));

- the set of the rate equations (Eqs. (11)–(12)) are related to well-established physical principles as the "reptation" model and the "Smoluchowski" theory of coagulation. It is important to point out that in the "Smoluchowski" theory of coagulation the effect of the Brownian motion is clearly taken into account;

- the thermodynamic consistence of the model was analyzed (Section 3);

- a theoretical criterium for the transition region based on the strain gradient mapping degeneration was discussed and exploited (Section 4), however it is important to stand out the necessity of more discussions and analysis on the relationships (Eqs. (48) and (56)) taking into account some additional characteristics (as temperature, ...) and their consequences. These characteristics shall be considered in future work goals;

- the illustrative numerical examples attest the capability of the model to predict the expected behavior of real thixotropic substances under some typical rheological tests (Section 5).

It is also important to comment that the developed ideas and presented in this work can be easily extended to approaches including more than two types of microstructure (related to each specific relaxation mechanism) that are taken into account in the constitutive equation system. It is clear that the complexity level of the considered substance determines the necessity of these incorporations. In this context, it can be noted the versatility of the approach exposed here, presenting some interesting perspectives on thixotropic modeling that can be more explored in future works.

Symbology

τ	shear stress
γ	shear strain
G	shear modulus
η	dynamic viscosity
λ	structural parameter
$\mathfrak{G}\dot{\gamma}$	functional associated to structural parameter time evolution
$\delta^{i\ldots}_{r\ldots}$	the generalized Kronecker delta
$\cdot$	total time derivative
$\cdot\cdot$	double total time derivative
$\odot$	Oldroyd time derivative
ν	associated to the Maxwellian mechanism
μ	associated to the pure viscous mechanism
$\bar{}$	first-order tensor
$\underline{=}$	second-order tensor
$\cdot$	inner product
:	double inner product

Author details

Hilbeth P. Azikri de Deus[1*] and Mikhail Itskov[2]

1 Nucleus of Applied and Theoretical Mechanics – NuMAT, UTFPR, Brazil

2 Department of Continuum Mechanics, RWTH – Aachen University, Germany

*Address all correspondence to: azikri@utfpr.edu.br

References

[1] Zhang X, Li W, Gong X. Thixotropy of MR shear-thickening fluids. Smart Materials and Structures. 2010; **19**(125012):1-6

[2] El-Gendy H, Alcoutlabi M, Jemmett M, Deo M, Magda J, Venkatesan R, Montesi A. The propagation of pressure in a gelled waxy oil pipeline as studied by particle imaging velocimetry. AICHE Journal. 2012;**58**(3):302-311

[3] Nguyen Q, Boger D. Thixotropic behaviour of concentrated bauxite residue suspensions. Rheologica Acta. 1985;**24**:427-437

[4] Mujumdar A, Beris AN, Metzner AB. Transient phenomena in thixotropic systems. Journal of Non-Newtonian Fluid Mechanics. 2002;**102**:157-178

[5] de Souza Mendes PR. Modeling the thixotropic behavior of structured fluids. Journal of Non-Newtonian Fluid Mechanics. 2009;**164**:66-75

[6] Swift DL, Friedlander SK. The coagulation of hydrosols by Brownian motion and laminar shear flow. Journal of Colloid Science. 1964;**19**: 621-647

[7] Yaghouti MR, Rezakhanlou F, Hammond A. Coagulation, diffusion and the continuous Smoluchowski equation. Stochastic Processes and their Applications. 2009;**119**:3042-3080

[8] Azikri de Deus HP, Negrão CRO, Franco AT. The modified Jeffreys model approach for elasto-viscoplastic thixotropic substances. Physics Letter A. 2016;**380**:585-595

[9] Hammond A, Rezakhanlou F. Kinetic limit for a system of coagulating planar Brownian particles. Journal of Statistical Physics. 2006;**124**:997-1040

[10] Niethammer B, Velázquez JJL. Self-similar solutions with fat tails for Smoluchowski's coagulation equation with locally bounded kernels. Communications in Mathematical Physics. 2013;**318**:502-532

[11] Pokrovskii VN. A justification of the reptation-tube dynamics of a linear macromolecule in the mesoscopic approach. Physica A. 2006;**366**:88-106

[12] Öttinger HC. A thermodynamically admissible reptation model for fast flows of entangled polymers. Journal of Rheology. 1999;**43**:1461-1493

[13] Mewis J. Thixotropy: A general review. Journal of Non-Newtonian Fluid Mechanics. 1979;**6**:1-20

[14] Barnes H. Thixotropy: A review. Journal of Non-Newtonian Fluid Mechanics. 1997;**70**:1-33

[15] Toorman EA. Modeling the thixotropic behaviour of dense cohesive sediment suspensions. Rheologica Acta. 1997;**36**:56-65

[16] Ritter RA, Batycky JP. Numerical prediction of the pipeline flow characteristics of thixotropic liquids. SPE Journal. 1967;**7**:369-376

[17] Dullaert K, Mewis J. A structural kinetics model for thixotropy. Journal of Non-Newtonian Fluid Mechanics. 2006; **139**:21-30

[18] de Souza Mendes PR. Thixotropic elasto-viscoplastic model for structured fluids. Soft Matter. 2011;**7**:2471-2483

[19] Azikri de Deus HP, Dupim GSP. Over strucutural nature of the thixotropic fluids behavior. Applied Mathematical Sciences. 2012;**6**: 6871-6889

[20] Azikri de Deus HP, Dupim GSP. On behavior of the thixotropic fluids. Physics Letters A. 2013;**337**:478-485

[21] Azikri de Deus HP, Dupim GSP. Some aspects over thixotropic fluid behavior. Advanced Materials Research. 2013;**629**:623-634

[22] Ardakani HA, Mitsoulis E, Hatzikiriakos SG. Thixotropic flow of toothpaste through extrusion dies. Journal of Non-Newtonian Fluid Mechanics. 2011;**166**:1262-1271

[23] Oliveira GM, Rocha LLV, Franco AT, Negrão COR. Numerical simulation of the start-up of Bingham fluid flows in pipelines. Journal of Non-Newtonian Fluid Mechanics. 2010;**165**:1114-1128

[24] Mewis J, Wagner NJ. Thixotropy. Advances in Colloid and Interface Science. 2009;**147–148**:214-227

[25] Dullaert K, Mewis J. Thixotropy: Build-up and breakdown curves during flow. Journal of Rheology. 2005;**49**(6): 1213-1230

[26] Potanin A. 3D simulations of the flow of thixotropic fluids, in large-gap Couette and vane-cup geometries. Journal of Non-Newtonian Fluid Mechanics. 2010;**165**:299-312

[27] Derksen JJ, Prashant NV. Simulations of complex flow of thixotropic liquids. Journal of Non-Newtonian Fluid Mechanics. 2009;**160**: 65-75

[28] Barnes HA. The yield stress – A review or 'panta rei' – Everything flows? Journal of Non-Newtonian Fluid Mechanics. 1999;**81**:133-178

[29] Patil PD, Feng JJ, Hatzikiriakos SG. Constitutive modeling and flow simulation of polytetrafluoroethylene (PTFE) paste extrusion. Journal of Non-Newtonian Fluid Mechanics. 2006;**139**: 44-53

[30] Marrucci G. The free energy constitutive equation for polymer solutions from the dumbell model. Transactions. Society of Rheology. 1972; **16**:321-330

[31] Marrucci G, Titomanlio G, Sarti GC. Testing of a constitutive equation for entangled networks by elongational and shear data of polymer melts. Rheologica Acta. 1973;**12**:269-275

[32] Silva TABP. Aálise do Módulo de Cisalhamento Associado a Modelo de Jeffreys Modificado (in Portuguese). Master Dissertation. UTFPR, PPGEM, Brazil; 2017

[33] Rajagopal KR, Srinivasa AR. On thermomechanical restrictions of continua. Proceedings of the Royal Society of London A. 2004;**406**:631-651

[34] Rajagopal KR, Srinivasa AR. Inelastic behavior of materials. I. Theoretical underpinnings. International Journal of Plasticity. 1998; **14**:945-967

[35] Rajagopal KR, Srinivasa AR. Inelastic behavior of materials II. Inelastic response. International Journal of Plasticity. 1998;**14**:967-995

[36] Rajagopal KR, Srinivasa AR. A thermodynamic framework for rate-type fluid models. Journal of Non-Newtonian Fluid Mechanics. 2000;**88**: 207-227

[37] Marze S, Guillermic RM, Saint-James A. Oscillatory rheology of aqueous foams: Surfactant, liquid fraction, experimental protocol and aging effects. Soft Matter. 2009;**5**(9): 1937

[38] Mohan L, Pellet C, Cloitre M, Bonnecaze R. Local mobility and microstructure in periodically sheared soft particle glasses and their connection to macroscopic rheology. Journal of Rheology. 2013;**57**(3):1023

[39] Mason TG, Bibette J, Weitz DA. Yielding and flow of monodisperse emulsions. Journal of Colloid and Interface Science. 1996;**179**(179): 439-448

[40] Souza Mendes PR, Thompson RL, Alicke AA, Leite RT. The quasilinear large-amplitude viscoelastic regime and its significance in the rheological characterization of soft matter. Journal of Rheology. 2014;**58**(2):537-561

[41] Walls HJ, Caines SB, Sanchez AM, Khan SA. Yield stress and wall slip phenomena in colloidal silica gels. Journal of Rheology. 2003;**47**(4):847

[42] Andrade DEV, Takii BA, Franco AT, Negrão CRO. The influence of the initial cooling condition on the flow curve of waxy crude oil. In: 15th Brazilian Congress of Thermal Sciences and Engineering. Belém: ABCM; 2014

[43] Divoux T, Barentin C, Manneville S. Stress overshoot in a simple yield stress fluid: An extensive study combining rheology and velocimetry. Soft Matter. 2011;**7**:9335-9349

[44] Fernandes RR, Andrade DEV, Franco AT, Negrão COR. Sampling methodology for rheological tests of drilling fluids: A study of the aging time and preshearing. In: 15th Brazilian Congress of Thermal Sciences and Engineering. Belém; 2014

[45] Knauss WG, Zhu W. Nonlinearly viscoelastic behavior of polycarbonate. I response under pure shear. Mechanics of Time-Dependent Materials. 2002;**6**: 231-269

[46] Agarwa DC. Tensor Calculus and Riemannian Geometry. Meerut, India: Krishna Prakashan Media Ltd.; 2007

[47] Lovelock D, Rund H. Tensors, Differential Forms, and Variational Principles. New York, USA: Dover Publications, INC.; 1989

[48] Seth BR. Elastic-plastic transition in shells and tubes under pressure. Journal of Applied Mathematics and Mechanics. 1963;**43**:345-351

[49] Seth BR. Generalized strain and transition concepts for elasti-plastic deformation, creep and relaxation. In: Proceedings of the Eleventh International Congress of Applied Mechanics; 1966. pp. 383–389

[50] Seth BR. Transition Concept in Continuum Mechanics. Corvallis, USA: Seminar Lectures delivered in Oregon State University (unpublished); 1968

[51] Purushothama CM. Elastic-plastic transition. Journal of Applied Mathematics and Mechanics. **45**: 401-408

[52] Morinigo V Jr. Verificação Teórico-numéica de Modelo Constitutivo Aplicado a Fluidos Tixotrópicos Compostos por Duas Estruturas Distintas (in Portuguese). TCC, Federal University of Technology-Paraná – UTFPR, Brazil; 2017